NJC

ROYAL SOCIETY OF CHEMISTRY

PAPER

View Article Online
View Journal | View Issue

Cite this: *New J. Chem.*, 2025, **49**, 3708

Columnar liquid-crystalline compounds based on phosphine oxide: effects of structures of the flexible chains on their self-assembling behavior†

Jingze Bi, [a] Junya Uchida [a] and Takashi Kato *[ab]

Received 31st December 2024,
Accepted 30th January 2025

DOI: 10.1039/d4nj05558f

rsc.li/njc

A series of liquid-crystalline compounds based on triphenylphosphine oxide incorporating alkene-terminated side chains were designed and synthesized to examine their self-assembling behavior and responsiveness to electric fields. All compounds exhibited rectangular columnar phases, with isotropization temperatures varying based on their molecular structures. The incorporation of alkene-terminated side chains into liquid crystals in this series resulted in improved electric field responsiveness, as evidenced by the formation of fully homeotropic alignment under both direct current and alternating current electric fields. These results provide valuable insights into the structure–property relationships governing the self-assembling behavior and electric field responsiveness of the polar columnar liquid crystals, offering design principles for the development of electric field responsive materials.

Introduction

The shape of liquid-crystalline (LC) molecules is a crucial factor as it fundamentally determines ordered molecular packing.[1–3] Traditionally, rod-like and disk-like molecules have been the basic shapes used in developing calamitic and discotic LC materials, respectively.[4–6] Among the LC materials with different shapes, LC materials with a C_3 symmetry are a fascinating class of compounds characterized by their unique molecular geometry and self-assembly properties.[7–18] These materials typically feature a central aromatic core with three identical arms extending outward, forming a star-like structure. The tuneable molecular design in aromatic cores and extending arms of the C_3-symmetric structure enables versatile control over self-assembling properties and potential applications.[12–21]

Our intention here is to develop polar liquid crystals with C_3-symmetric structure.[9,14] The study of polar columnar liquid crystals remains in its early stage, while the extensive researches have been conducted on a variety of calamitic liquid crystals with polar group.[22–26] In polar columnar liquid crystals, strong π–π stackings between molecules can increase viscosity, which results in lower responsiveness to electric fields (*E*-fields). In 1993, Swager reported on vanadyl salicylaldehyde Schiff base compounds as polar columnar liquid crystals.[27] These compounds were designed to mimic the well-known ferroelectric material, barium titanium(IV) oxide ($BaTiO_3$).[27] Since then, some of polar columnar liquid crystals including the development of cone-like,[28,29] bowl-like,[30,31] taper-like,[32–34] sulfone-based,[35] and hydrogen-bonded molecules[36–39] have been reported. However, these polar columnar structures are associated with relatively high driving voltages and low response speeds when subjected to an external *E*-field.

Numerous methods have been employed to fabricate LC materials with higher *E*-field responsiveness, such as reducing the viscosity and increasing the dielectric anisotropy of LC materials.[22–26] As the introduction of alkene side chains to liquid crystals resulting in a decrease of the melting and isotropization temperatures,[40–43] the fluidity of these liquid crystals therefore greatly enhanced. For instance, introducing alkene-terminated side chains to the polymer dispersed liquid crystal (PDLC) film results in a higher contrast ratio and faster response time.[43]

In this work, we aim to enhance the *E*-field responsiveness of triphenylphosphine oxide (TPPO)-based liquid crystals, which have already demonstrated to be *E*-field responsive in our previous work.[14] The cone-shaped polar structures of these TPPO-based molecules suggest potential for molecular reorientation or inversion under moderate *E*-field conditions. Enhanced *E*-field responsiveness in these compounds could facilitate their application in high-density memory devices and other electronic applications, potentially improving device performance through more efficient molecular switching.

[a] *Department of Chemistry and Biotechnology, School of Engineering, The University of Tokyo, Hongo, Bunkyo-ku, Tokyo, 113-8656, Japan*
E-mail: kato@chiral.t.u-tokyo.ac.jp
[b] *Institute for Aqua Regeneration, Shinshu University, Wakasato, Nagano, 380-8553, Japan*

† Electronic supplementary information (ESI) available. See DOI: **https://doi.org/10.1039/d4nj05558f**

Results and discussion

Material design

To enhance the *E*-field responsiveness of TPPO-based compounds, a series of molecules were designed and synthesized by incorporating alkene-terminated side chains (Fig. 1 and 2). Compared to LC molecules having fully saturated alkyl chains, LC molecules with alkene groups demonstrate enhanced responsiveness under external *E*-field.[44–46] In addition to ether linkages, amide linkages binding the TPPO core and side chains were also incorporated to examine their effects on LC properties and *E*-field responsiveness (Fig. 1 and 2). This structural variation allows us to investigate how different linking groups influence the self-assembly behaviour and responsiveness of these TPPO-based compounds.

Compound **1** has one alkoxy side chains and two alkene-terminated side chains at each arm, while compound **2** changed all the alkoxy side chains to alkene-terminated side chains (Fig. 2). These modifications were implemented to enhance *E*-field responsiveness compared to the reference compound **4**[9,14] with fully saturated alkoxy side chains (Fig. 2). In compound **3**, we replaced the ether linkages with amide groups while maintaining a side chain distribution similar to compound **1**, anticipating potential *E*-field induced reorientation through hydrogen-bonded structures.

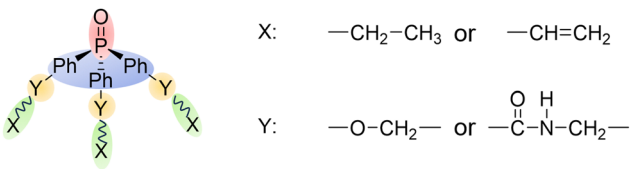

Fig. 1 Schematic illustration of molecular design.

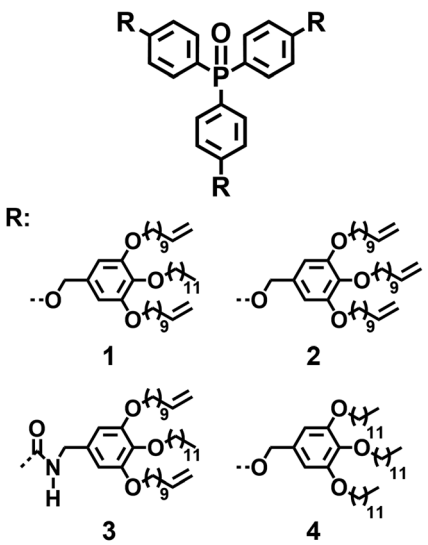

Fig. 2 Molecular structures of compounds **1–4**.

LC properties of the TPPO-based compounds with alkene-terminated side chains

The LC properties of compounds **1–3** were examined using polarizing optical microscopy (POM), differential scanning calorimetry (DSC), and X-ray diffraction (XRD) measurements (Fig. 3–5). The phase transition behavior of these compounds and compound **4**[14] is summarized in Table 1.

Compound **1** exhibited a focal conic texture which is typical for columnar phase (Fig. 3a). The DSC curves of **1** (Fig. 3b) showed only one peak at 28.9 °C corresponding to phase transition from a columnar phase to an isotropic phase during heating. On the cooling process, this compound maintained its columnar phase without crystallization. The XRD pattern of compound **1** (Fig. 3c) in the rectangular columnar phase displayed three distinct peaks at 34.6 Å, 31.6 Å, and 15.8 Å, assigned to the (110), (200), and (400) reflections, respectively.

Compound **2** showed a focal conic texture with smaller domains under crossed Nicols conditions at 15 °C during cooling (Fig. 4a). The DSC curves of **2** (Fig. 4b) showed a single transition peak at 24.8 °C, indicating the columnar-to-isotropic phase transition during heating. On the cooling process, this compound remained in the columnar phase from 14.7 °C to lower temperatures. Moreover, the isotropization temperature

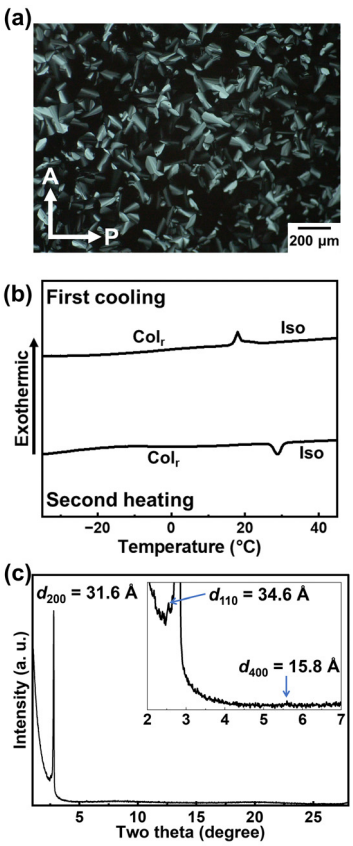

Fig. 3 (a) Polarizing optical microscopy image at 20 °C on cooling from the isotropic phase, (b) differential scanning calorimetry thermograms, and (c) X-ray diffraction patterns of compound **1** at 20 °C. Vertical and horizontal white arrows shown in (a) indicate the analyzer and polarizer directions, respectively.

Table 1 Thermal properties of TPPO-based LC compounds

Compound	Phase transition behavior[a]				
1			Col_r	28.9 (1.4)	Iso
2			Col_r	24.8 (1.4)	Iso
3			Col_r	94.4 (1.1)	Iso
4[14]	Cr	2.5 (12.8)	Col_r	56.0 (2.1)	Iso

[a] Phase transition temperature (°C) and transition enthalpy (kJ mol^{-1}) in parentheses, deduced by DSC upon the second heating at a scanning rate of 5 K min^{-1}. Col_r: rectangular columnar phase; Iso: isotropic phase; Cr: crystalline phase.

of **2** was lower than that of **1**. These results suggest that the incorporation of alkene-terminated side chains in TPPO-based compounds disrupted ordered molecular packing. The XRD pattern of compound **2** (Fig. 4c) in the rectangular columnar phase showed three peaks at 34.0 Å, 30.7 Å, 15.4 Å, corresponding to the (110), (200) and (400) reflections, respectively.

A similar focal conic texture was observed under POM for compound **3** (Fig. 5a), which incorporated both

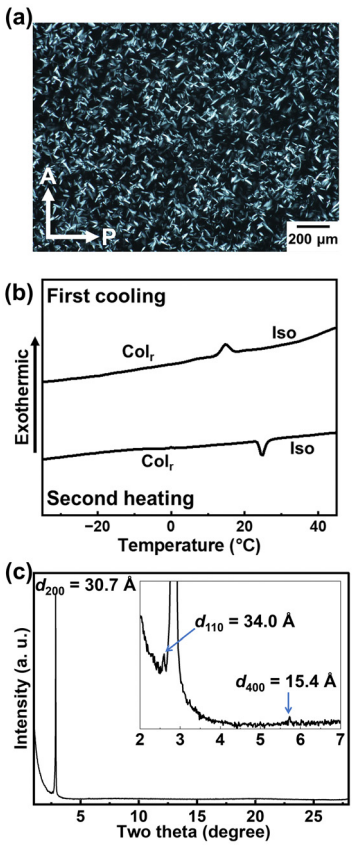

Fig. 4 (a) Polarizing optical microscopy image at 15 °C on cooling from the isotropic phase, (b) differential scanning calorimetry thermograms, and (c) X-ray diffraction patterns of compound **2** at 20 °C. Vertical and horizontal white arrows shown in (a) indicate the analyzer and polarizer directions, respectively.

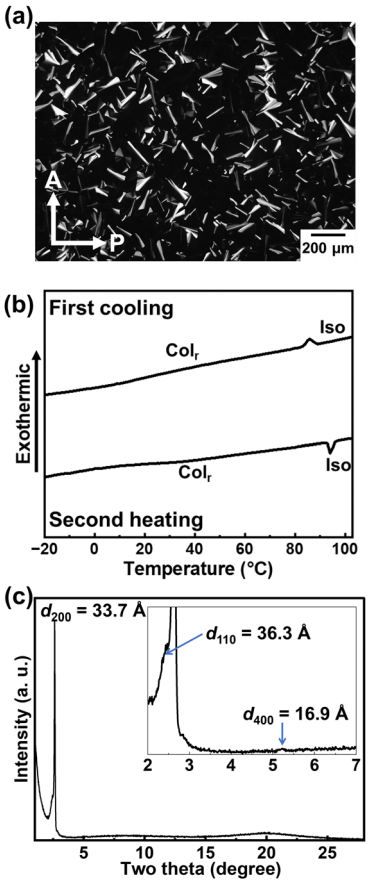

Fig. 5 (a) Polarizing optical microscopy image at 20 °C on cooling from the isotropic phase, (b) differential scanning calorimetry thermograms, and (c) X-ray diffraction patterns of compound **3** at 20 °C. Vertical and horizontal white arrows shown in (a) indicate the analyzer and polarizer directions, respectively.

alkene-terminated side chains and amide linkages. However, the isotropization temperature was significantly increased to 94.4 °C upon heating (Fig. 5b). As the formation of intermolecular hydrogen bonds was confirmed by the Fourier-transform infrared (FT-IR) spectra (Fig. S1, ESI†), this increase of isotropization temperature is primarily attributed to the formation of intermolecular hydrogen bonds,[21] which greatly enhance the order of molecular packing. The XRD pattern (Fig. 5c) exhibited three peaks at 36.3 Å, 33.7 Å and 16.9 Å, corresponding to the (110), (200) and (400) reflections, respectively.

The isotropization temperatures of compounds **1** and **2** were lower than that of compound **4** (Table 1) probably due to the less ordered molecular packing caused by alkene-terminated side chains. Although compound **3** also possesses alkene-terminated side chains, formation of the intermolecular hydrogen bond through the amide linkage results in a higher isotropization temperature than compound **4**.

E-field responsiveness of the TPPO-based compounds with alkene-terminated side chains

The *E*-field responsiveness of these TPPO-based compounds was evaluated using both direct current (DC) and alternating

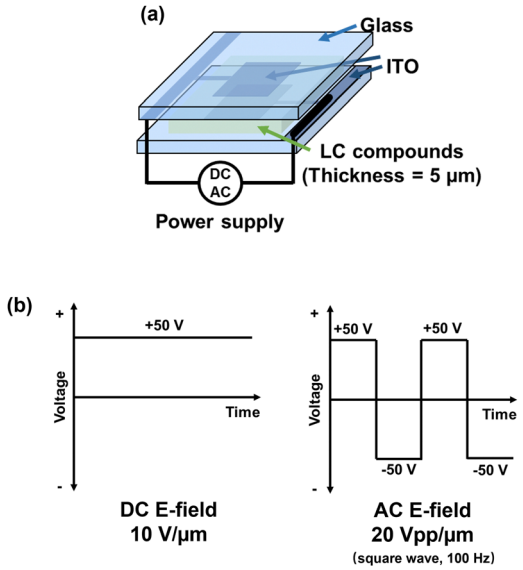

Fig. 6 (a) Schematic setup for electric field responsiveness measurements. (b) Amplitudes of direct current and alternating current electric fields.

current (AC) *E*-fields applied during controlled thermal treatment. The LC cells were first heated above their respective isotropization temperatures and then cooled at a rate of 5 °C min^{-1} to 10 °C under applied *E*-fields (Fig. 6a). For systematic comparison, the voltage of *E*-field was set at 10 V μm^{-1} for DC and 20 Vpp μm^{-1} (square wave, 100 Hz) for AC to make sure that all the compounds are under uniform conditions (Fig. 6b). These *E*-field parameters were selected to ensure comparable experimental conditions while maintaining field strengths sufficient to induce molecular reorientation without causing LC material degradation.

Under both DC and AC *E*-fields, compound **4**, containing only saturated alkoxy side chains, maintained its polydomain texture under both field conditions, indicating insufficient molecular reorientation to achieve homeotropic alignment (Fig. 7a).

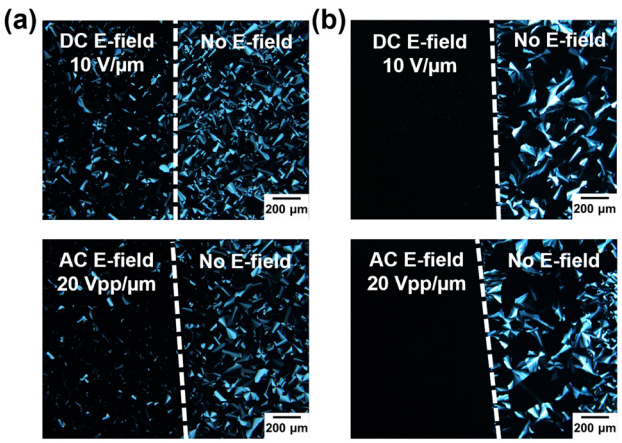

Fig. 7 Polarizing optical microscopy images of compounds (a) **4** and (b) **1** after applying direct current and alternating current electric fields. The dashed lines represent the borders of electric field operating and non-operating parts.

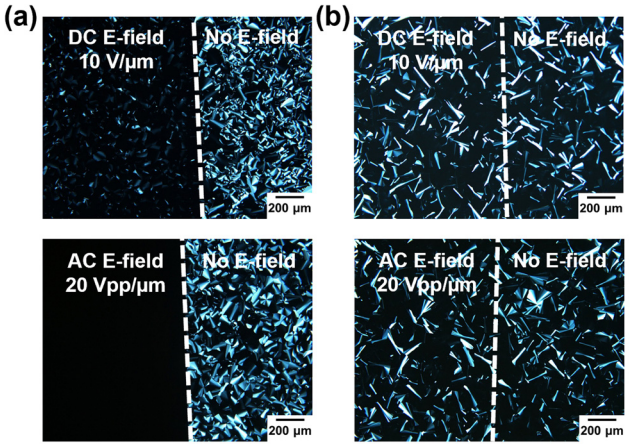

Fig. 8 Polarizing optical microscopy images of compounds (a) **2** and (b) **3** after applying direct current and alternating current electric fields. The dashed lines represent the borders of electric field operating and non-operating parts.

In contrast, compound **1**, incorporating six alkene-terminated side chains, exhibited complete transformation from polydomain to homeotropic alignment, evidenced by the disappearance of birefringent textures under both DC and AC *E*-fields (Fig. 7b). These results confirmed that the introduction of alkene-terminated side chains increased the *E*-field responsiveness of TPPO-based liquid crystals. The increased *E*-field responsiveness of **1** compared to that of **4** may be ascribed to the increased molecular mobility and the decreased viscosity. These phenomena were observed for calamitic liquid crystals.[40–43]

For TPPO-based compound **2** with three additional alkene-terminated side chains, this compound showed similar homeotropic alignment under an AC *E*-field (Fig. 8a). Nevertheless, under a DC *E*-field, the focal conic texture still existed (Fig. 8a), suggesting that the *E*-field responsiveness of this compound was different from compound **1** with fewer alkene-terminated side chains. We propose that homeotropic alignments are easier to achieve under AC *E*-fields due to the rapid field alternation allowing both parallel and antiparallel dipole orientations (Fig. S2, ESI†). The *E*-field responsiveness of compound **1** can be attributed to its optimized balance between molecular mobility and ordered packing, while compound **2** has a lower isotropization temperature indicating disrupted molecular packing (Table 1).

Compound **3**, incorporating both alkene-terminated side chains and amide linkages, showed remarkable resistance to *E*-field induced reorientation, maintaining its original texture under both DC and AC *E*-fields (Fig. 8b). These results indicate that compound **3** lacks *E*-field responsiveness under these conditions.

Effect of dipoles moments on the *E*-field responsiveness of the TPPO-based liquid crystals

To further elucidate the origin of the differences in *E*-field responsiveness, analogues of compounds **1** and **3** were subjected to molecular modelling to calculate their dipole

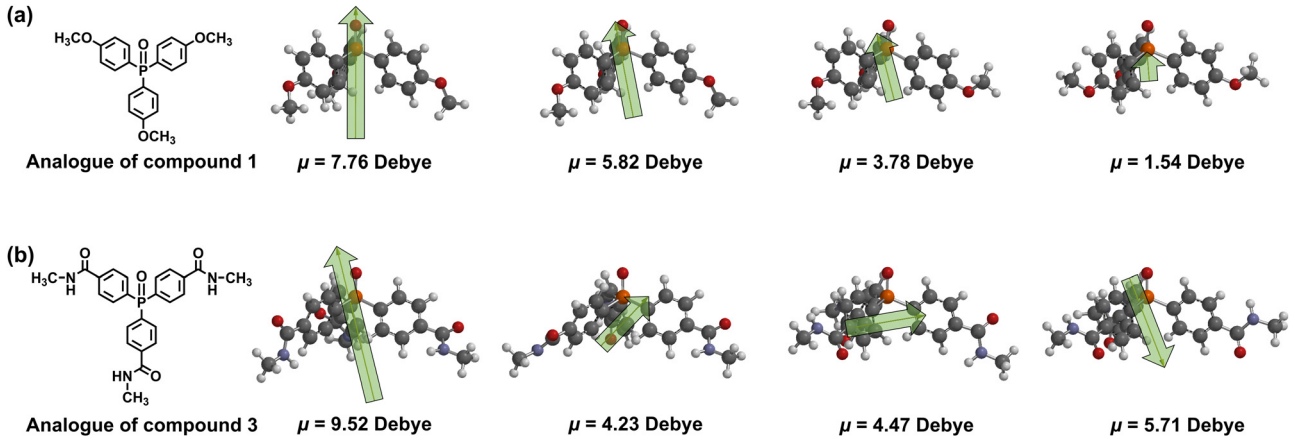

Fig. 9 Molecular structures and energy minimized structures of analogues of (a) compound **1** and (b) compound **3**. Green arrows indicate the directions of dipole moments.

moments (Fig. 9). The analogue of compound **1** exhibited four distinct conformational states with dipole moments of 7.76, 5.82, 3.78, and 1.54 debye, arising from different orientations of the ether bonds (Fig. 9a). Despite the variation in magnitude, these dipole moments maintained consistent alignment along the phosphine oxide group. The unidirectional alignment of the dipole moments may cause the homeotropic alignment of the columnar LC assembly of **1** under the *E*-fields (Fig. 7b). In contrast, the analogue of compound **3** displayed four conformational states with dipole moments of 9.52, 4.23, 4.47, and 5.71 debye, originating from different conformations of the amide bonds (Fig. 9b). Notably, these dipole moments showed diverse orientations: some almost perpendicular to phosphine oxide group and others along it. This orientational disorder of dipole moments in compound **3** may result in the formation of polydomain LC structure under the *E*-fields (Fig. 8b), despite individual conformations showing comparable or even higher dipole moments than compound **1**. These results highlight the crucial role of not only the magnitude but also the directional alignment of molecular dipoles in determining the *E*-field responsiveness of columnar liquid crystals.

Conclusions

In this work, LC materials based on TPPO cores were designed and synthesized with alkene-terminated side chains to enhance their *E*-field responsiveness. All compounds self-assembled into rectangular columnar phases, with the introduction of alkene-terminated side chains enhancing *E*-field responsiveness, as evidenced by the achievement of homeotropic alignment. Molecular modelling studies revealed that the incorporation of amide linkages in compound **3** resulted in misaligned molecular dipoles that significantly diminished *E*-field responsiveness, despite having similar alkene-terminated side chains as compound **1**. These findings highlight the critical balance between molecular mobility, self-assembled structure, and dipole alignment in designing *E*-field responsive materials, providing valuable guidance for future development of advanced LC materials.

Experimental

Preparation of LC compounds

Compounds **1** and **2** were synthesized *via* a Williamson ether reaction of tris(4-hydroxyphenyl) phosphine oxide with a fan-shaped benzyl chloride derivative possessing one alkoxy chain and two alkene-terminated alkoxy chains, or three alkene-terminated alkoxy chains (Scheme S1, ESI†). Compound **3** was synthesized by amide condensation using a fan-shaped amine derivative possessing one alkoxy chain and two alkene-terminated alkoxy chains with tris(4-carboxylphenyl) phosphine oxide (Scheme S2, ESI†). Compound **4** was prepared according to a procedure reported previously[9,14] and used as a reference compound for comparative analysis of LC properties and *E*-field responsiveness. Full synthetic details and characterization data for compounds **1–3** are provided in the ESI.†

Preparation of LC cells and *E*-field responsiveness experiments

LC cells were prepared by introducing compounds **1–4** in their isotropic phases followed by cooling to the LC phases. The LC cells were then connected to a power supply using copper wires, placed on a hot stage using Kapton tape, and observed under POM. The *E*-field responsiveness experiments were conducted under 50 V DC and 100 Vpp AC to ensure that all LC cells were subjected to 10 V μm^{-1} DC and 20 Vpp μm^{-1} AC *E*-fields, respectively.

Density functional theory calculation

Molecular modelling was performed by density functional theory (DFT) calculation at the B3LYP/6-31G* level with a wavefunction Spartan 18 (v. 1. 4. 4) program. Analogues of compounds **1** and **3** were used for computational efficiency by replacing the fan-shaped groups with methyl groups while maintaining the essential TPPO core structure.

Author contributions

T. K. conceived the concept and materials design. T. K., J. B., and J. U. designed the molecules and synthetic protocols. J. B.

performed the syntheses, POM, DSC, XRD, and FT-IR characterizations. T. K., J. B., and J. U. wrote the manuscript. All the authors discussed the results.

Data availability

The data supporting this article have been included as part of the ESI.†

Conflicts of interest

There are no conflicts to declare.

Acknowledgements

This work was supported by JSPS KAKENHI Grant Number JP19H05715, JST CREST Grant Number JPMJCR19Q1, and JST SPRING Grant Number JPMJSP2108.

Notes and references

1 D. Demus, J. W. Goodby, G. W. Gray, H.-W. Spiess and V. Vill, *Handbook of Liquid Crystals*, Wiley-VCH, Weinheim, 1998.
2 T. Kato, J. Uchida, T. Ichikawa and T. Sakamoto, *Angew. Chem., Int. Ed.*, 2018, **57**, 4355–4371.
3 M. Funahashi and T. Kato, *Liq. Cryst.*, 2015, **42**, 909–917.
4 J. Uchida, B. Soberats, M. Gupta and T. Kato, *Adv. Mater.*, 2022, **34**, 2109063.
5 T. Wöhrle, I. Wurzbach, J. Kirres, A. Kostidou, N. Kapernaum, J. Litterscheidt, J. C. Haenle, P. Staffeld, A. Baro, F. Giesselmann and S. Laschat, *Chem. Rev.*, 2016, **116**, 1139–1241.
6 R. J. Bushby and K. Kawata, *Liq. Cryst.*, 2011, **38**, 1415–1426.
7 M. Lehmann, in *Handbook of Liquid Crystals*, ed. J. W. Goodby, P. J. Collings, T. Kato, C. Tschierske, H. Gleeson, P. Raynes and V. Vill, Wiley-VCH, Weinheim, 2014, vol. 5, pp. 243–315.
8 M. Lehmann, in *Liquid Crystals: Materials Design and Self-Assembly*, ed. C. Tschierske, Springer, Berlin, Heidelberg, 2012, pp. 193–223.
9 T. Hatano and T. Kato, *Chem. Commun.*, 2006, 1277–1279.
10 N. Tober, T. Rieth, M. Lehmann and H. Detert, *Chem. – Eur. J.*, 2019, **25**, 15295–15304.
11 M. Lambov, N. Hensiek, A.-C. Pöppler and M. Lehmann, *ChemPlusChem*, 2020, **85**, 2219–2229.
12 L.-L. Lai, S.-J. Hsu, H.-C. Hsu, S.-W. Wang, K.-L. Cheng, C.-J. Chen, T.-H. Wang and H.-F. Hsu, *Chem. – Eur. J.*, 2012, **18**, 6542–6547.
13 A. Sandeep, V. K. Praveen, D. S. S. Rao, S. K. Prasad and A. Ajayaghosh, *ACS Omega*, 2018, **3**, 4392–4399.
14 J. Bi, A. Akiyama, J. Uchida, K. Kishikawa and T. Kato, *ACS Appl. Polym. Mater.*, 2024, **6**, 676–683.
15 L. Liu, J. Li, H. Zhu, H. Yang, X. Feng, D. Xiao, Y. Yang and H. Gao, *J. Mater. Chem. C*, 2024, **12**, 6450–6456.
16 T. Yasuda, T. Shimizu, F. Liu, G. Ungar and T. Kato, *J. Am. Chem. Soc.*, 2011, **133**, 13437–13444.
17 K. Tanabe, T. Yasuda and T. Kato, *Chem. Lett.*, 2008, **37**, 1208–1209.
18 M. Kimura, T. Hatano, T. Yasuda, J. Morita, Y. Akama, K. Minoura, T. Shimomura and T. Kato, *Chem. Lett.*, 2009, **38**, 800–801.
19 J. De, S. P. Gupta, S. S. Swayamprabha, D. K. Dubey, I. Bala, I. Sarkar, G. Dey, J.-H. Jou, S. Ghosh and S. K. Pal, *J. Phys. Chem. C*, 2018, **122**, 23659–23674.
20 E. Beltrán, J. L. Serrano, T. Sierra and R. Giménez, *J. Mater. Chem.*, 2012, **22**, 7797–7805.
21 A. Martínez-Bueno, R. Vidal, J. Ortega, J. Etxebarria, C. L. Folcia, R. Giménez and T. Sierra, *Mater. Today Chem.*, 2023, **29**, 101394.
22 P. Raynes, in *Handbook of Liquid Crystals*, ed. J. W. Goodby, P. J. Collings, T. Kato, C. Tschierske, H. Gleeson, P. Raynes and V. Vill, Wiley-VCH, Weinheim, 2014, vol. 8, pp. 3–20.
23 S. Lagerwall, in *Handbook of Liquid Crystals*, ed. J. W. Goodby, P. J. Collings, T. Kato, C. Tschierske, H. Gleeson, P. Raynes and V. Vill, Wiley-VCH, Weinheim, 2014, vol. 8, pp. 213–234.
24 T. Kato, H. Kihara, T. Uryu, S. Ujiie, K. Iimura, J. M. J. Fréchet and U. Kumar, *Ferroelectrics*, 1993, **148**, 161–167.
25 M. Bremer, P. Kirsch, M. Klasen-Memmer and K. Tarumi, *Angew. Chem., Int. Ed.*, 2013, **52**, 8880–8896.
26 H. Nishikawa, K. Shiroshita, H. Higuchi, Y. Okumura, Y. Haseba, S. Yamamoto, K. Sago and H. Kikuchi, *Adv. Mater.*, 2017, **29**, 1702354.
27 A. G. Serrette and T. M. Swager, *J. Am. Chem. Soc.*, 1993, **115**, 8879–8880.
28 M. Sawamura, K. Kawai, Y. Matsuo, K. Kanie, T. Kato and E. Nakamura, *Nature*, 2002, **419**, 702–705.
29 D. Kilian, D. Knawby, M. A. Athanassopoulou, S. T. Trzaska, T. M. Swager, S. Wróbel and W. Haase, *Liq. Cryst.*, 2000, **27**, 509–521.
30 S. Furukawa, J. Wu, M. Koyama, K. Hayashi, N. Hoshino, T. Takeda, Y. Suzuki, J. Kawamata, M. Saito and T. Akutagawa, *Nat. Commun.*, 2021, **12**, 768–776.
31 Y. Matsuo, A. Muramatsu, R. Hamasaki, N. Mizoshita, T. Kato and E. Nakamura, *J. Am. Chem. Soc.*, 2004, **126**, 432–433.
32 H. Shimura, M. Yoshio, A. Hamasaki, T. Mukai, H. Ohno and T. Kato, *Adv. Mater.*, 2009, **21**, 1591–1594.
33 T. Kato, T. Yasuda, Y. Kamikawa and M. Yoshio, *Chem. Commun.*, 2009, 729–739.
34 D. Miyajima, F. Araoka, H. Takezoe, J. Kim, K. Kato, M. Takata and T. Aida, *Angew. Chem., Int. Ed.*, 2011, **50**, 7865–7869.
35 M. Yoshio, R. Konishi, T. Sakamoto and T. Kato, *New J. Chem.*, 2013, **37**, 143–147.
36 H. Takezoe, K. Kishikawa and E. Gorecka, *J. Mater. Chem.*, 2006, **16**, 2412–2416.
37 Y. Okada, S. Matsumoto, Y. Takanishi, K. Ishikawa, S. Nakahara, K. Kishikawa and H. Takezoe, *Phys. Rev. E: Stat., Nonlinear, Soft Matter Phys.*, 2005, **72**, 020701.

38 K. Kishikawa, S. Nakahara, Y. Nishikawa, S. Kohmoto and M. Yamamoto, *J. Am. Chem. Soc.*, 2005, **127**, 2565–2571.
39 A. V. Gorbunov, T. Putzeys, I. Urbanavičiūtė, M. Wübbenhorst, R. P. Sijbesma and M. Kemerink, *Phys. Chem. Chem. Phys.*, 2016, **18**, 23663–23672.
40 C. K. Lee, S. S. Kwon, S. T. Shin, E. J. Choi, S. Lee and L. C. Chien, *Liq. Cryst.*, 2002, **29**, 1007–1013.
41 S. Zhu, Y. Zhu, J. Chigan, Y. Fu, Q. Weng, X. Niu, W. Chen, R. Chen, X. Chen and Z. An, *Liq. Cryst.*, 2019, **46**, 2149–2158.
42 V. Percec and M. Lee, *Macromolecules*, 1991, **24** 1017–1024.
43 H. Zhang, T. Zhong, M. Chen, L. Zhang, X. Liu, H. Cao, H. Yang and S. Zhu, *Liq. Cryst.*, 2018, **45**, 1118–1128.
44 M. Schadt, M. Petrzilka, P. R. Gerber and A. Villiger, *Mol. Cryst. Liq. Cryst.*, 1985, **122**, 241–260.
45 M. Schadt, R. Buchecker and A. Villiger, *Liq. Cryst.*, 1990, **7**, 519–536.
46 J. W. Goodby, *Liq. Cryst.*, 2011, **38**, 1363–1387.

